Surface-phonon dispersion curves and the longitudinal resonance in Ag(001) observed by helium-atom scattering

N. Bunjes, N. S. Luo, P. Ruggerone,* J. P. Toennies, and G. Witte
Max-Planck-Institut für Strömungsforschung, Bunsenstrasse 10, D-37073 Göttingen, Germany
(Received 4 April 1994)

An intense longitudinal-surface-phonon resonance in addition to the Rayleigh mode is observed on Ag(001) by inelastic helium-atom scattering (HAS). This mode, which is only barely visible by electron-energy-loss spectroscopy, is similar to the one previously detected by HAS for Cu(001). This observation provides additional evidence for the pseudocharge model previously invoked to explain the anomalous longitudinal resonance observed in several metal surfaces by HAS. The observed differences between Cu(001) and Ag(001) are also shown to be consistent with the pseudocharge model.

In recent years, the experimental techniques of helium-atom scattering (HAS) (Ref. 1) and electron-energy-loss spectroscopy (EELS) (Ref. 2) have provided a large amount of information on the surface-vibrational properties of metals. Surface-phonon-dispersion curves and scattering-intensity data furnished by the two spectroscopies have stimulated theoretical interest in the dynamics at surfaces. The anomalous surface-longitudinal resonance (L) first found on the close-packed (111) noble-metal surfaces by HAS (Refs. 3,4) was later confirmed by EELS.[5] However, the inability of Born–von Karman force constant models to explain both the large intensities in the HAS time-of-flight (TOF) spectra and the dispersion curves called attention to shortcomings in the force constant models.[4,6,7] Recent HAS-TOF data on Cu(001),[7] which showed that the longitudinal resonance is up to five times more intense than the Rayleigh mode (R), whereas the same mode is not seen in EELS points to a different sensitivity of the two techniques. The pseudocharge model which incorporates the electronic degrees of freedom[4,8] into the lattice dynamics in addition to providing a more satisfactory description of the dispersion curves than models also explains the large HAS response of the longitudinal mode in this system.[7] A somewhat related model has also been recently introduced to explain the Cu(001) HAS data.[9] Whereas electrons in the impact regime are scattered mainly by the tightly bound core electrons, which rigidly follow the motion of the surface ions, helium atoms according to the pseudocharge model are inelastically scattered by the electron density at the Fermi level as deformed by the atomic motion of surface phonons. Thus HAS and EELS are in fact nicely complementary as they can probe the amplitudes of the electron density at the surface and of the nuclei for each single phonon, respectively. As a result of these developments the electronic response to the nuclear motion which is basic to an understanding of the lattice dynamics of metals is accessible to study.

In this paper, we present HAS measurements of surface-phonon-dispersion curves for Ag(001) along both symmetry directions of the surface Brillouin zone. As in Cu(001), the TOF spectra show large differences in the relative intensity of the low-lying longitudinal resonance with respect to the Rayleigh mode. Along the $\langle 100 \rangle$ direction ($\bar{\Gamma}\bar{M}$) the corresponding peak is as much as twice as intense as the Rayleigh wave peak, whereas in the $\langle 110 \rangle$ direction ($\bar{\Gamma}\bar{X}$) the longitudinal resonance is weaker than the Rayleigh mode. As in the case of copper the relative strength of the longitudinal resonance on the (001) silver surface is larger than on the (111) surface.[3] EELS measurements of the Rayleigh wave dispersion curves along both symmetry directions are in agreement with the HAS measurements within the EELS experimental error.[10–12] In the EELS spectra[10,11] there is, however, only very weak evidence for a longitudinal mode at the $\bar{M}$ point. In addition to these modes, first-principle calculations[11] predict a first-layer longitudinal resonance at the $\bar{X}$ point and a resonance at the $\bar{M}$ point, the frequencies of which lie only about 0.4 meV above the Rayleigh mode. These modes cannot be resolved in the EELS experiments and lie below the longitudinal resonance seen in the experiments reported on here. As in the case of copper, calculations based on the Born–von Karman force constant model carried out in our laboratory are not able to account for the observed mode nor for the large HAS intensities. The same pseudocharge model as successfully used for Cu(111) (Ref. 4) and Cu(001) (Ref. 7) can explain both the dispersion curves and the large intensity of the longitudinal resonance in terms of the deformations of the conduction electrons at the surface. The comparison between the HAS experimental data on both Cu(001) and Ag(001) provides important new insight into differences in the dynamical electronic response at the surface of the two metals.

The pseudocharge multipolar expansion scheme, is only described briefly here, since a more accurate description can be found in Ref. 4. The approach is based on a partition of the electronic charge density over a set of N special points $\{\mathbf{r}_{lj}\}$ $(j=1,\ldots,N)$ within each unit cell l, by performing a multipolar expansion centered at every $\{\mathbf{r}_{lj}\}$, each one representing a pseudocharge. The expansion coefficients in the multipolar representation act in the lattice dynamics as electronic degrees of freedom. As for the Cu fcc crystal we have chosen $N=6$ with the charges located between each set of nearest-neighbor atoms and the multipole series is terminated at the quadrupole term. The dipolar and quadrupolar deformations of the electronic charge density are dynamically coupled to the ionic displacements to account for the many-body effects in the phonon dispersion curves. Five coupling parameters are sufficient to fit all the bulk phonon features as well as the measured elastic constants and to

account for the deviations from the Cauchy relation. Only two have to be modified to fit the surface-phonon-dispersion curves.

The helium scattering apparatus used in this experiment has been described in detail elsewhere.[13] Essentially, it consists of a supersonic He nozzle-beam source, a target chamber, and a time-of-flight drift tube followed by a detector consisting of an electron bombardment ionizer and a mass spectrometer. The beam energy spread ($\Delta E/E$) is about 2%. TOF techniques were used to analyze the energy of the scattered helium atoms at an angle of 90° to the incident beam. The Ag(001) crystal was oriented to better than 0.25° and then prepared by mechanical polishing followed by cycles of sputtering with 850-eV Ar^+ ions for 90 min at 400 K and annealing at 700 K for 2 min at UHV conditions. X-ray photoelectron spectroscopy showed no impurities above 0.5% of the monolayer detection limit.

In order to reduce the multiphonon scattering most of the TOF spectra were recorded with an incident-beam energy of 24.4 meV ($k_i = 6.8$ Å^{-1}) at a crystal temperature of 150 K. Under these conditions the intensity of the first-order diffraction peak relative to the specular is 2.9×10^{-3} for the ⟨110⟩ direction and 1.6×10^{-4} for the ⟨100⟩ direction, respectively. By comparison, for the ⟨110⟩ direction the relative intensity for Cu(001) was only 3×10^{-5} while for the ⟨100⟩ direction no diffraction peak could be detected, indicating that the Ag(001) surface is definitely more corrugated than that of Cu(001).

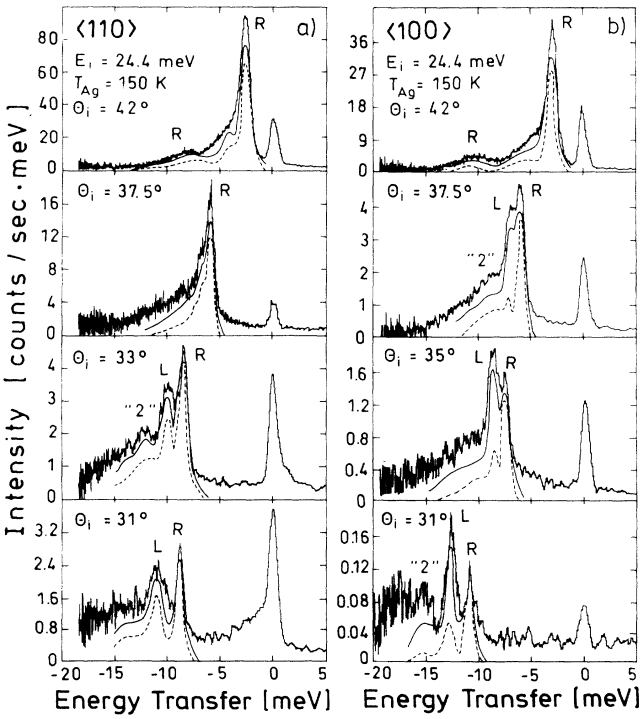

FIG. 1. Series of HAS time-of-flight spectra measured along (a) the ⟨110⟩ and (b) the ⟨100⟩ azimuths. The temperature of the crystal is 150 K and the energies of the incident beam are 24.4 meV. R marks the Rayleigh wave, while L labels the longitudinal resonance. The dashed lines are the simulated TOF spectra which are calculated with only the ion core contributions, while the solid lines denote the results of the pseudocharge calculations.

Figure 1 shows two series of TOF spectra out of a total of more than 350 spectra taken along (a) (⟨110⟩) $\bar{\Gamma}\bar{X}$ and (b) (⟨100⟩) $\bar{\Gamma}\bar{M}$. In both directions, besides the elastic peak due to defects, two well-resolved energy-loss structures are observed. One is attributed to the Rayleigh wave and the second one at higher-energy losses is attributed to a surface resonance. In the ⟨110⟩ direction the L peaks are consistently smaller than the R peaks. In the other direction, the ratio between the intensities of the two features changes as the zone boundary is approached with the L peaks becoming twice as large as the Raleigh-wave peaks. In addition to the R and L peaks a weak shoulder, labeled by a 2, which was first seen on Al(001) (Ref. 14) and recently carefully analyzed in Cu(001) (Ref. 15) can be seen in some of the spectra.

The measured surface-dispersion curves along the border of the irreducible part of the surface Brillouin zone are compared with calculations based on the pseudocharge model in Fig. 2. The open circles are the HAS data, while the EELS points[10–12] are marked with solid symbols. The few HAS points, labeled by a 2, appear to coincide with the bulk band edges. The EELS Rayleigh wave frequency lies about 1 meV below the HAS data, but the difference is within the EELS experimental error. The solid lines show the pseudocharge model surface modes and the resonances, both of which are in good agreement with all the experimental data.

The phonon frequencies of the surface modes at $\bar{X}$ and $\bar{M}$ measured by both HAS and EELS are compared with the results of embedded-atom molecular-dynamics calculations,[16] *ab initio* calculations,[11] and with the results of the present pseudocharge calculations in Table I. The pseudocharge model provides the best description of all the available experimental data. The agreement between experiment and theory for the shear horizontal mode S_1 found only by EELS is also not very good for the other approaches listed in Table I. Furthermore, all the calcula-

TABLE I. Comparison of experimental and theoretical surface phonon frequencies (in meV) at the zone boundaries for Ag(001).

	HAS[a]	EELS	EAM (Ref. 16)	*Ab initio* (Ref. 11)	Pseudocharge model[a]
$\bar{X}$ S_1 (SH)		3.3 (Ref. 12)	6.4	5.8	7.4
S_4 (R)	9.1	8.7 (Refs. 10 and 11)	8.7	8.7	9.1
L	12.2		9.7	9.1	12.2
S_6			16.3	17.0	17.5
$\bar{M}$ S_1 (R)	11.5	10.2 (Ref. 10)	11.5	10.3	11.2
S_2[b]				13.2–14.1	
L		11.5 (Ref. 10)	14.1	13.6	14.7

[a]Present work.

[b]This mode is characterized by a dominant second-layer normal displacement.

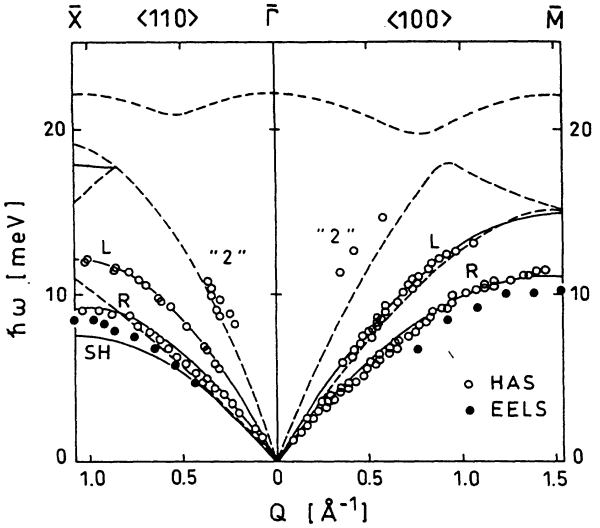

FIG. 2. The phonon-dispersion curves on Ag(001) calculated with the pseudocharge model. The solid lines are surface modes and resonances, while the dashed lines are the bulk band edges. The open circles indicate the HAS data and the closed circles are the EELS measurements (Refs. 10–12).

tions predict a phonon feature in the optical gap at $\bar{X}$, labeled S_6, which although present in the EELS data for Cu(001) has not been detected in EELS experiments on Ag(001), probably because of the very small EELS cross section.[11]

The values of the pseudocharge coupling parameters obtained from a best fit of the bulk and surface-phonon-dispersion curves are listed in Table II, together with the copper coupling constants for both the bulk and the (001) surface. A good fit of the surface-dispersion curves is obtained with the pseudocharge model by only changing the dipolar (C) and quadrupolar (B) coupling parameters (see Table II) as in the case of Cu(001). As expected, the same overall trend in the surface induced changes of the parameters is present in both cases. Compared to the bulk values the reduction of the dipole–nearest-neighbor (NN) ion coupling parameter (B in Table II) and the increase of the quadrupolar-NN ion term (C in Table II) is smaller in silver than for copper.[17] As discussed below these differences are consistent with differences in the electronic surface properties.

As already outlined in Ref. 4, the dynamic coupling of the He atom to the deformations of the pseudocharges can be accounted for by assuming a linear dependence of the potential on the charge density, as proposed by Esbjerg and Nørskov.[18] Therefore, in the expression for the inelastic He atom scattering cross section, the additional force contributions from the dipolar and quadrupolar deformations of the pseudocharges f_d and f_q (Ref. 4) are added to the force f_a of the He atoms coupling to the ion cores. Thus the scattering cross section is proportional to $|f_a+f_d+f_q|^2$ (see Ref. 4) instead of being proportional to $|f_a|^2$ as in the previous theory.[19]

The simulated TOF spectra are compared with the experiments in Figs. 1(a) and 1(b) for the two symmetry directions. The dashed lines are the results of the simulation with only the contribution to the scattering cross section due to the ionic displacements. The positions of the peaks are in good agreement with the experiments, but whereas the Rayleigh wave peak intensities are rather well explained, these calculations cannot reproduce the relatively large intensity of the longitudinal resonance. The solid lines show the results of a simulation in which the coupling additional force contributions f_d and f_q of the He atoms to the pseudocharge deformations are included. The agreement between the measured and calculated intensities is now remarkably good and in particular the large enhancement of the longitudinal resonance along the $\bar{\Gamma}\bar{M}$ direction is well reproduced.

The difference with the (111) situation and the anisotropy was already easily explained within the pseudocharge scheme in Ref. 7 and is only briefly sketched here. As the zone boundary is approached, neighboring ions acquire an antiphase motion in the longitudinal mode which squeezes out the intercalated electron charge density. The resulting deformations are z polarized and they couple very strongly with the impinging He atoms, which are sensitive to changes in the electronic charge density at 3–4 Å above the surface plane. On the contrary, the R-peak intensity is hardly affected by the presence of the pseudocharges, since the zone-boundary antiphase z motions produce only a slight deformation of the pseudocharges compared to the charge-density changes at the core positions. Along ⟨100⟩ the surface ions move in a longitudinal motion parallel to the line connecting

TABLE II. Comparison of best-fit lattice-dynamics coupling parameters from the pseudocharge model and He-surface interaction potential parameters for bulk and (001)-surface silver and copper.

	Coupling parameter	units	Bulk Ag	Bulk Cu[a]	Ag	Cu[a]
A	ion-NN ion	N/m	24.65	28.6	24.6	28.6
B	dipole-NN ion	N/m	2.46	1.10	1.66	0.12
C	quadrupole NN ion	N/m	12.17	7.80	18.2	17.4
H	dipole–second-NN ion	N/m	1.99	2.50	1.99	2.50
F	quadrupole–second-NN ion	N/m	2.19	2.40	2.19	2.40
A_{eff}	effective NN force	N/m	24.4	30.5	18.8	21.2
α_{dip}	dipolar polarizability	10^{-24} cm^3	1.62	2.26	3.0	17.3
α_{quad}	quadrupolar polarizability	10^{-40} cm^5	1.51	2.1	1.95	2.75

[a]Taken from Ref. 4.

second-nearest neighbors and thus have a greater vibration amplitude than in the ⟨110⟩ direction where the motion is inhibited by nearest-neighbor ions inducing larger deformations of the pseudocharges. The smaller enhancement of the longitudinal resonance at the (111) surface[3] also observed for copper[4,7] is also consistent with a theoretical prediction of a smaller increase of the electronic charge at the surface with respect to the bulk than at the (001) surface.[20] Thus, the more dramatic increase in the TOF peak intensity of the longitudinally polarized mode on the (001) surface is a consequence of the different electron density response on this surface.

The smaller enhancement of the longitudinal resonance on Ag(001) compared to Cu(001) is consistent with what is known about differences in the electronic structures of the two surfaces of these two noble metals. Theoretical support for the pseudocharge enhancement of the longitudinal resonance intensity comes from the charge transfer from the *d* bands into the *sp* bands at the Cu surface as discussed by Kleinman.[20] The *sp* charge density, which is predominant at the Fermi level in the noble metals is of importance since it couples strongest to the impinging helium atom. This *sp* charge density is expected to be less for Ag than for Cu. For Ag(001) the presence of a strongly surface localized *sp* state above the Fermi level is still under discussion,[21] but in any case the amount of charge associated with it is very small. For Cu(001) this state has been clearly detected in several experiments and predicted by theoretical calculations.[20,22] Moreover we note that the work function for Ag(001) is 4.64 eV,[23] slightly larger than the 4.59-eV value of Cu(001). As a result the amplitude of the tails of the Cu(001) wave functions are expected to be somewhat larger than for Ag(001) at the same distance in the range 3–4 Å above the surface, where the turning point of the helium atom is located. This difference is also consistent with the observed smaller diffraction intensities of the Cu(001) surface indicating a smoother surface in the case of copper. Additional support comes from Kevan *et al.*[24] and Freeman and co-workers[21] who argue that spin-orbit interaction enhances the *s-d* hybridization in Ag(001), thus reducing the *sp* contribution. This is in accord with the smaller polarizabilities at the Ag surface with respect to Cu as estimated from the pseudocharge model (see Table II).

In summary, the HAS experiments on Ag(001) give additional experimental evidence for the pseudocharge model which assumes a dynamical coupling between the probe particles and the surface vibrations, produced by the phonon induced deformations of the conduction electrons. This interpretation is confirmed by the results of the TOF simulations calculated in the framework of the pseudocharge model. The smaller enhancements in the longitudinal resonance on the Ag(001) surface compared to Cu(001) is shown to be consistent with what is known about the electronic structures of the two surfaces.

N.S.L and P.R. gratefully acknowledge the support of the Max-Planck Society. The authors thank G. Benedek (Milan), V. Celli (Virginia), J. R. Manson (Clemson), and L. Kleinman (Austin) for many valuable critical discussions.

---

*Present address: Fritz-Haber-Institut, Faradayweg 46, D-14195 Berlin-Dahlem, Germany.

[1]J. P. Toennies, in *Solvay Conference on Surface Science,* edited by F. de Wette, Springer Series in Surface Sciences Vol. 14 (Springer, Heidelberg, 1988), p. 248.

[2]H. Ibach, J. Vac. Sci. Technol. A **5**, 419 (1987).

[3]U. Harten, J. P. Toennies, and Ch. Wöll, Faraday Discuss. Chem. Soc. **80**, 137 (1985); R. B. Doak, U. Harten, and J. P. Toennies, Phys. Rev. Lett. **51**, 578 (1983).

[4]C. Kaden, P. Ruggerone, J. P. Toennies, G. Zhang, and G. Benedek, Phys. Rev. B **46**, 13 509 (1992); C. Kaden, P. Ruggerone, J. P. Toennies, and G. Benedek, Nuovo Cimento D **14**, 627 (1992).

[5]M. H. Mohamed, L. L. Kesmodel, B. M. Hall, and D. L. Mills, Phys. Rev. B **37**, 2763 (1988); B. M. Hall, D. L. Mills, M. H. Mohamed, and L. L. Kesmodel, Phys. Rev. B **38**, 5856 (1988); D. L. Mills (private communication).

[6]J. P. Toennies, Superlatt. Microstruct. **7**, 193 (1990).

[7]G. Benedek, J. Ellis, N. S. Luo, A. Reichmuth, P. Ruggerone, and J. P. Toennies, Phys. Rev. B **48**, 4917 (1993).

[8]C. S. Jayanthi, H. Bilz, W. Kress, and G. Benedek, Phys. Rev. Lett. **59**, 795 (1987).

[9]D. Cvetko, F. Floreano, A. Lausi, A. Morgante, M. Peloi, F. Tommasini, T. Zambelli, V. Bortolani, A. Franchini, and G. Santoro, J. Electron Spectrosc. Relat. Phenom. **64/65**, 671 (1993).

[10]Y. Chen, S. Y. Tong, M. Rocca, P. Moretto, U. Valbusa, K. P. Bohnen, and K. M. Ho, Surf. Sci. Lett. **250**, L389 (1991).

[11]Y. Chen, S. Y. Tong, Jae-Sung Kim, L. L. Kesmodel, T. Rodach, K. P. Bohnen, and K. M. Ho, Phys. Rev. B **44**, 11 394 (1991).

[12]J. L. Erskine, E.-J. Jeong, J. Yater, Y. Chen, and S. Y. Tong, J. Vac. Sci. Technol. A **8**, 2649 (1990).

[13]B. J. Hinch, A. Lock, H. H. Madden, J. P. Toennies, and G. Witte, Phys. Rev. B **42**, 1547 (1990).

[14]A. Franchini, V. Bortolani, G. Santoro, V. Celli, A. G. Eguiluz, J. A. Gaspar, M. Gester, A. Lock, and J. P. Toennies, Phys. Rev. B **47**, 4691 (1993).

[15]F. Hofmann, J. R. Manson, and J. P. Toennies, J. Chem. Phys. (to be published).

[16]L. Yang, T. S. Raman, and M. S. Daw, Phys. Rev. B **44**, 13 725 (1991).

[17]In retrospect it appears as if the value previously reported for *B* for Cu(001) (Ref. 4) may be too small.

[18]N. Esbjerg and J. K. Nørskov, Phys. Rev. B **45**, 807 (1980).

[19]V. Bortolani and A. C. Levi, Riv. Nuovo Cimento **9**, 1 (1986).

[20]L. Kleinman, Phys. Rev. B **26**, 1055 (1982); L. Kleinman (private communication).

[21]H. Erschbaumer, A. J. Freeman, C. L. Fu, and R. Podloucky, Surf. Sci. **243**, 317 (1991).

[22]F. J. Arlinghaus, J. G. Gay, and J. R. Smith, Phys. Rev. B **23**, 5152 (1981).

[23]H. Hölzl and F. K. Schulte, in *Solid Surface Physics,* edited by Editors (Springer, Berlin, 1979), and references therein.

[24]S. D. Kevan, N. G. Stoffel, and N. V. Smith, Phys. Rev. B **32**, 4956 (1985).